QCD ANALYSIS OF STRUCTURE FUNCTIONS OF REAL AND VIRTUAL PHOTONS a

I. Schienbein

Institut für Physik, Universität Dortmund D-44221 Dortmund, Germany E-mail: schien@hal1.physik.uni-dortmund.de

Parameter–free and perturbatively stable leading order (LO) and next–to–leading order (NLO) parton densities for real and virtual photons are presented.

1 Introduction

The hadronic structure of real and virtual photons can be measured in electron positron scattering processes in which one lepton serves as a source of target photons with virtuality $P^2 << Q^2$ where Q^2 is the virtuality of the probing photon. The measured e^+e^- cross section can then be obtained by a convolution of a flux of target photons with the deep inelastic electron (positron) photon scattering cross section which is (completely analogous to the case of deep inelastic electron proton scattering) described by two structure functions $F_{2,L}$. In the QCD importoned parton model the photon structure functions $F_{2,L}^{(p^2)}(x,Q^2)$ are given by a convolution of non-perturbative parton densities of the (real or virtual) photon with appropriate perturbatively calculable short distance coefficient functions. The photonic parton distributions are governed by inhomogenous evolution equations which have to be supplemented with appropriate boundary conditions.

Here we briefly describe recently proposed parameter–free leading order (LO) and next–to–leading order (NLO) boundary conditions for real and virtual photons 1 .

2 Boundary Conditions

The boundary conditions are given in the DIS $_{\gamma}$ scheme at a low resolution scale $Q_0^2 \approx 0.3 \text{ GeV}^2$. The exact LO and NLO values of the universal (i. e. hadron–independent) input scale Q_0 are fixed by the experimentally well constrained radiative parton densities of the proton ².

^aTalk given at the DIS-2000 conference, Liverpool, 25-30 April 2000

2.1 Real Photon

The boundary conditions for the real photon ¹ are given by a vector meson dominance (VMD) ansatz where (at the low scale Q_0) the physical photon is assumed to be a coherent superposition of vector mesons which have the same quantum numbers as the photon

$$f^{\gamma}(x,Q_0^2) = f_{had}^{\gamma}(x,Q_0^2) = \alpha G_f^2 f^{\pi^0}(x,Q_0^2) \tag{1}$$

with $G_{u,d}^2=(g_\rho\pm g_\omega)^2$ and $G_g^2=G_s^2=g_\rho^2+g_\omega^2$ $(g_\rho^2=0.50,\,g_\omega^2=0.043)$. This optimal coherence maximally enhances the up quark which is favoured by the experimental data.

Since parton distributions of vector mesons $(\rho, \omega, ...)$ are experimentally undetermined, we furthermore assume that these are similar to pionic parton distributions. Thus, for given pionic parton distributions our model has no free parameter.

2.2 Pion

Since only the pionic valence density is experimentally rather well known, we utilize a constituent quark model 3 to relate the pionic light sea and gluon to the much better known parton distributions of the proton 2 . In Mellin-n-space one easily finds the following boundary conditions for the pion distribution functions 4,5

$$g^{\pi}(n, Q_0^2) = \frac{v^{\pi}}{v^p} g^p, \qquad \bar{q}^{\pi}(n, Q_0^2) = \frac{v^{\pi}}{v^p} \bar{q}^p,$$
 (2)

which only depend on the rather well determined valence distribution of the pion and the parton distributions of the proton.

2.3 Virtual Photon

In the virtual photon case we propose the following boundary conditions which of course smoothly extrapolate to the real photon case $(P^2 \to 0)^1$:

$$f^{\gamma(P^2)}(x,Q^2=\tilde{P}^2)=f_{\rm had}^{\gamma(P^2)}(x,\tilde{P}^2)=\eta(P^2)f_{\rm had}^{\gamma}(x,\tilde{P}^2)\,. \eqno(3)$$

The employed dipole suppression factor (rho-meson propagator) $\eta(P^2) = (1 + P^2/m_\rho^2)^{-2}$ is somewhat speculative and can be regarded as the simplest choice of modelling the P^2 -suppression.

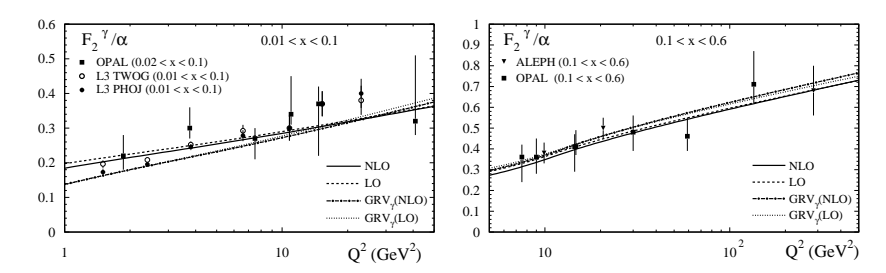


Figure 1: F_2^{γ}/α in dependence of Q^2 for two different x-bins.

3 Numerical results

The presented model successfully describes LEP data on the photon structure function F_2^{γ} and H1 dijet data. For details see Ref. ¹ and references therein. As an example, in Fig. 1 the evolution of F_2 with Q^2 is shown for two different x-bins. Also shown are the GRV_{γ} predictions ⁶. For 0.1 < x < 0.6 all curves are close together because this x-range is already dominated by the point-like solution, whereas for 0.01 < x < 0.1 our results are larger at small values of Q^2 and evolve weaklier with Q^2 due to the different boundary conditions.

Acknowledgments

Supported in part by the Graduiertenkolleg 'Erzeugung und Zerfälle von Elementarteilchen' of the Deutsche Forschungsgemeinschaft at the Universität Dortmund and by the Bundesministerium für Bildung, Wissenschaft, Forschung und Technologie, Bonn.

References

- 1. M. Glück, E. Reya, and I. Schienbein, *Phys. Rev.* D **60**, 054019 (1999).
- 2. M. Glück, E. Reya, and A. Vogt, Eur. Phys. J. C 5, 461 (1998).
- 3. G. Altarelli, N. Cabibbo, L. Maiani, and R. Petronzio, *Nucl. Phys.* B **69**, 531 (1974).
- 4. M. Glück, E. Reya, M. Stratmann, Eur. Phys. J. C 2, 159 (1998).
- 5. M. Glück, E. Reya, I. Schienbein, Eur. Phys. J. C 10, 313 (1999).
- M. Glück, E. Reya, and A. Vogt, Phys. Rev. D 45, 3986 (1992); ibid. D 46, 1973 (1992).